Article

Minimum Number of Experimental Data for the Thermal Characterization of a Hot Water Storage Tank

María Gasque [1], **Federico Ibáñez** [2] **and Pablo González-Altozano** [2,*]

1 Departamento de Física Aplicada, Universitat Politècnica de València, Camino de Vera s/n, 46022 Valencia, Spain; mgasque@fis.upv.es
2 Departamento de Ingeniería Rural y Agroalimentaria, Universitat Politècnica de València, Camino de Vera s/n, 46022 Valencia, Spain; fedeibso@gmail.com
* Correspondence: pgaltozano@agf.upv.es

Abstract: This paper demonstrates that it is possible to characterize the water temperature profile and its temporal trend in a hot water storage tank during the thermal charge process, using a minimum number of thermocouples (TC), with minor differences compared to experimental data. Four experimental tests (two types of inlet and two water flow rates) were conducted in a 950 L capacity tank. For each experimental test (with 12 TC), four models were developed using a decreasing number of TC (7, 4, 3 and 2, respectively). The results of the estimation of water temperature obtained with each of the four models were compared with those of a fifth model performed with 12 TC. All models were tested for constant inlet temperature. Very acceptable results were achieved (*RMSE* between 0.2065 °C and 0.8706 °C in models with 3 TC). The models were also useful to estimate the water temperature profile and the evolution of thermocline thickness even with only 3 TC (*RMSE* between 0.00247 °C and 0.00292 °C). A comparison with a CFD model was carried out to complete the study with very small differences between both approaches when applied to the estimation of the instantaneous temperature profile. The proposed methodology has proven to be very effective in estimating several of the temperature-based indices commonly employed to evaluate thermal stratification in water storage tanks, with only two or three experimental temperature data measurements. It can also be used as a complementary tool to other techniques such as the validation of numerical simulations or in cases where only a few experimental temperature values are available.

Keywords: thermal energy storage; experimental tests; water temperature evolution; thermocline thickness; thermal stratification; charge process

1. Introduction

Thermal applications of solar energy have become widespread, and solar water heating systems, used mainly for domestic and industrial purposes, have become widely used. In these facilities, due to the high irregularity and discontinuity of both the energy source and the hot water demand, a hot water storage tank (HWST) is essential [1].

Temperature stratification within a water tank is highly desirable, and its enhancement and maintenance lead to improving the efficiency of thermal storage and, therefore, the system performance. Many studies have dealt with the assessment and characterization of water stratification. In this regard, the reviews [2–4] address and discuss the more relevant and innovative experimental and numerical studies performed to evaluate, measure and favor thermal stratification within an HWST.

In studies based on experimental tests, the characterization of the temperature profile inside the tank and its evolution over time was required to properly perform the analysis of the spatial temperature field and evaluate the thermal performance of the tank [5–7]. Thus, the installation of evenly distributed, multiple temperature sensors is quite usual in experimental tests, with the disadvantage of providing discrete temperature data.

Concerning numerical approaches, many simulation studies are proposed in the literature for the purpose of characterizing and improving thermal performance in a water storage tank. Thus, [3,8], among others, provided a comprehensive overview of the numerical studies that contributed to the current state of the art of thermal storage systems, many of which were carried out with computational fluid dynamics (CFD) techniques. Among the more recent numerical studies, Bouhal et al. [9] performed 2D-CFD simulations to assess the thermal stratification in an HWST and the impact of flate plates position within a tank. Moncho-Esteve et al. [10] implemented a 3D-CFD model to study the flow field and thermal stratification during charging. Once validated, the model was used to accomplish slight modifications of the inlet devices with the intention of optimizing system efficiency. Wang et al. [11] designed a novel equalizer and performed a 3D-CFD model, studying the influence of operating parameters on thermal stratification. In Chandra and Matuska [8], various CFD models were developed and proved that tank working conditions during the dynamic cycle can be optimized by proper selection of the inlet device. These investigations gave rise to valuable results since they allowed the prediction and analysis of fluid behavior and thermal performance in the storage tank with high spatial and temporal resolution, especially three-dimensional CFD techniques [12]. However, the CFD approach has the drawback of requiring the use of high computational resources and time, even if a one-dimensional CFD model is used [13,14]. A compromise must, therefore, be established between accuracy and computational time and resources. On the other hand, numerical models must necessarily be evaluated and validated against experimental tests, which, in turn, must have a sufficient number of measurement points.

Many methods and parameters were proposed to estimate stratification efficiency or to evaluate the level of stratification during the dynamic/static mode [15–18]. Some of these methods are based on determining the thermocline gradient or the thickness of the thermocline region [15], which, in a stratified thermal storage tank, is the region of steepest temperature gradient separating the hot and cold fluid zones [19] and is a common indicator of the effectiveness of stratification [20]. In this matter, the degree of stratification was evaluated in terms of thermocline thickness in several studies, both in chilled water energy storage [21–24] and in hot water tanks [11,14,25,26], as the same phenomenon occurs in both types of thermal storage tank systems, although the charge and discharge flow directions are reversed [19].

With the aim of avoiding the limitations and drawbacks of discrete temperature measurements in experimental tests, González-Altozano et al. [27] developed a new method called Virtual TC (VTC) that allows the estimating of water temperature at any depth and at any time in a storage tank during the charging process. The suitability of the methodology proposed was verified with its application to determine the instantaneous temperature profile and also to estimate the thermocline thickness and its evolution over time during thermal charging. The results obtained with these applications were comparatively analyzed against those obtained by linear interpolation. In this way, its effectiveness was demonstrated under experimental conditions.

The present study attempts to evaluate the sensitivity of the VTC procedure to the decrease in the number of temperature data points employed. It is also intended to verify the minimum amount of experimental temperature data (the number of thermocouples used) that allows to instantly estimate the temperature at any point without affecting the accuracy or the quality of the results.

The assessment of the reliability of the method is carried out by applying it to the estimation of both the instantaneous temperature profile and the thermocline thickness evolution throughout the charge cycle, using a decreasing number of measurement points. This study also attempts to demonstrate that the models implemented with fewer measurement points are suitable for the analysis of thermal performance and the determination of several of the temperature-based thermal stratification indices.

The study is completed with a comparison between the VTC method when using fewer measurement points and a numerical 3D-CFD approach, previously developed

and validated in [10] with the same storage tank and experimental tests. Specifically, a comparison is made between the results obtained with the two methods when applied to the estimation of the instantaneous temperature profile.

2. Research Background

In this section, the key issues of the VTC method are reviewed.

2.1. Experimental Tests

A series of experimental thermal charging tests were carried out in a facility provided with a 905 L capacity cylindrical HWST (0.8 m inner diameter and 1.8 m in height). Two separate inlets were arranged at the top of the tank symmetrical with respect to its vertical axis: an elbow inlet (E) and a conical diffuser made of sintered bronze (CD). The water tank temperature was measured with 12 T-type (Class 1) thermocouples (TC) evenly spaced in depth. The experimental facility, inlet devices and their operation, control and data acquisition system are described in more detail in García-Marí et al. [28]. Table 1 depicts the different tests conducted with the two inlet devices, E and CD, at two water flow rates, high (16 L/min) and low (6 L/min), which corresponds to a related fluid velocity of 1.92 m/h and 0.72 m/h, respectively. The Reynolds number (Re) at the inlet devices, determined from the inlet velocity, the diameter equivalent to the inlet section and the kinematic viscosity of water at a temperature of 52.2 °C, are also shown. The tests were conducted at a constant water flow rate until 120% of the total storage tank volume was replaced. Charge duration was expressed as a dimensionless time (t*).

Table 1. Experimental tests carried out.

|	Test Designation	Flow Rate (L/min)	Re (-)
Conical Diffuser inlet at Low flow rate	CDL	6	1898.6
Conical Diffuser inlet at High flow rate	CDH	16	5062.9
Elbow inlet at Low flow rate	EL	6	9183.4
Elbow inlet at High flow rate	EH	16	24,489.1

2.2. Modelling of Water Temperature Evolution and the VTC Method

To model the evolution of water temperature during the charge cycle at each of the 12 TC locations, the five-parameter logistic (5PL) function was chosen. Some other previous studies suggested a logistic cumulative distribution function to describe the behavior of a thermocline storage tank [29] or to assess the vertical temperature inside an HWST [14].

The high accuracy in the temperature evolution estimation with the 5PL curve allowed the interpolation of each parameter at any intermediate depth between two successive TC using the cubic spline. In this way, as many additional curves as desired may be interpolated between each pair of real consecutive thermocouples at the locations where there is no real thermocouple (virtual thermocouples). It is then possible to obtain the temperature profiles at any time and depth in a storage tank during the charging process, leaving aside the disadvantages derived from the availability of discrete temperature data [27].

2.3. Applying VTC. Determination of Some Temperature-Dependent Stratification Indices

To reinforce the validity of this methodology and highlight its advantages over other methods, the thermocline thickness evolution throughout the charge cycle estimated by applying VTC to the CDL and CDH tests are compared in Figure 1 with that obtained when using the 5PL, the four-parameter logistic function (4PL) and the linear interpolation (LI).
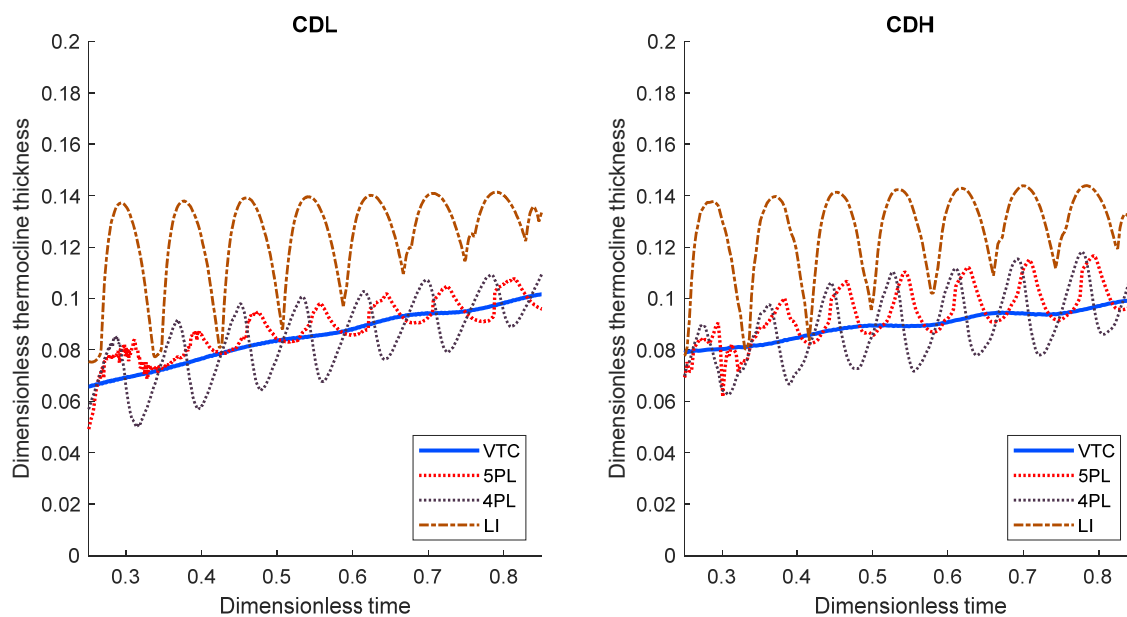
Figure 1. Dimensionless thermocline thickness evolution determined by Virtual TC (VTC), five parameter logistic function (5PL), four-parameter logistic function (4PL) and linear interpolation (LI) during the thermal charge process through the CD inlet at low flow rate (CDL, left side) and high flow rate (CDH, right side).

Although the thermocline thickness evolution is estimated from the experimental measurements provided by 12 TC in all cases, the results obtained by LI, 4PL and 5PL show a characteristic oscillation, the amplitude of this oscillation being greater in the case of LI. This oscillation, not appreciated when the estimation is made with VTC, is due to the temperature sensors providing discontinuous temperature data, although the temperature is a continuous parameter. Consequently, the thermocline thickness value determined by LI, 4PL or 5PL depends on the given time at which it is estimated. Additionally, the frequency of oscillation depends directly on the number of TC. The larger the number of TC employed, the higher the oscillation frequency, which reduces estimation errors. For this reason, the thermocline thickness estimated with the VTC method (using the same number of TC as the rest of the methods but considering a much larger number of temperature values in total) presents a much more uniform pattern. Specifically, in this study, 177 temperature values are used with the VTC method (12 real TC and 165 virtual TC) compared to the 12 temperature values used in the LI, 4PL and 5PL cases.

Thermocline thickness values of greater magnitude are obtained when estimated by LI rather than by the other methods. This is a consequence of the error made in considering the temperature variation between two consecutive TC (which are relatively far apart) as being linear. The evolution of the thermocline thickness determined from 4PL and 5PL oscillates around that obtained by VTC, presenting a similar trend in both cases, although the oscillation is less with 5PL. This oscillation increases the uncertainty in the punctual determination of the thermocline thickness and gives a clear advantage to the VTC method over the rest of the methods by showing a uniform pattern throughout the thermal charging process.

With the E inlet at a low flow rate, similar results are obtained to those with the CD inlet. Conversely, with the E inlet at a high flow rate, no method (LI, 4PL, 5PL or VTC) provides acceptable results owing to the turbulence generated at the inlet, which causes the mixing of the water inside the water tank. However, these are not the usual operating conditions in an HWST, where stratification is generally favored. Therefore, under the normal operating conditions of water storage tanks, the VTC method allows the thermocline thickness evolution to be obtained throughout the thermal charge process with more spatial precision and temporal stability than other methods. Similar conclusions can be drawn related to the

determination of other temperature-based parameters used to assess thermal stratification under the same operating conditions.

3. Materials and Methods

3.1. Sensitivity of the VTC Method to the Decrease in the Experimental Temperature Data Points Used

To assess the sensitivity of the method to reducing the number of temperature data points used, the VTC procedure was applied in the four charge tests (Table 1) to model the evolution of temperature at the points where the 12 TC were located but using the data provided by a smaller number of them.

In this way, for each of the experimental tests, four models were developed with the data recorded by 7, 4, 3 and 2 TC in the positions shown in Figure 2. The adjustment for temperature prediction in these four models was performed by extrapolating the parameters of the 5PL function to the location of the rest of the TC not used (points where real experimental data were available). The results were compared with a model conducted for each experimental test with the data provided by the 12 TC. Therefore, five models were performed for each test, resulting in a total of 20 models.
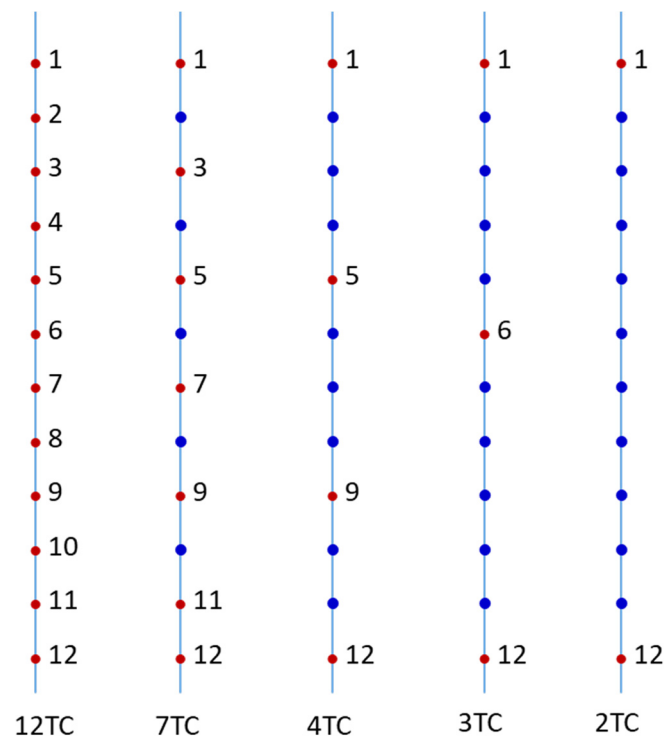
Figure 2. Number and position of the thermocouples used in the 5 models performed for each experimental test to evaluate the sensitivity of the VTC method to the number of TC used. The red circles represent the TC used, and the blue circles represent the positions at which the temperature prediction was made in each model.

Table 2 shows a summary of the models carried out in this study, including the number and location of the TC employed in each case and the model designation.

As discussed in García-Marí et al. [28], when the elbow inlet at a high flow rate is used, the effect of the flow rate negatively affects stratification, and the greater flow rate translates into greater turbulence leading to a higher degree of water mixing during thermal charging of the tank. Nevertheless, the EH test, as well as the models developed from it (MEH models), are included in the present study because they represent the limit case to establish the correct operation of the method.

Table 2. Models performed to analyze the sensitivity of the VTC method to the number of TC used.

Inlet Device	Flow Rate	Number of TC Used	Model Designation	TC Location
CD	L	12	MDL-12	1, 2, 3, 4, 5, 6, 7, 8, 9, 10, 11, 12
		7	MDL-7	1, 3, 5, 7, 9, 11, 12
		4	MDL-4	1, 5, 9, 12
		3	MDL-3	1, 6, 12
		2	MDL-2	1, 12
CD	H	12	MDH-12	1, 2, 3, 4, 5, 6, 7, 8, 9, 10, 11, 12
		7	MDH-7	1, 3, 5, 7, 9, 11, 12
		4	MDH-4	1, 5, 9, 12
		3	MDH-3	1, 6, 12
		2	MDH-2	1, 12
E	L	12	MEL-12	1, 2, 3, 4, 5, 6, 7, 8, 9, 10, 11, 12
		7	MEL-7	1, 3, 5, 7, 9, 11, 12
		4	MEL-4	1, 5, 9, 12
		3	MEL-3	1, 6, 12
		2	MEL-2	1, 12
E	H	12	MEH-12	1, 2, 3, 4, 5, 6, 7, 8, 9, 10, 11, 12
		7	MEH-7	1, 3, 5, 7, 9, 11, 12
		4	MEH-4	1, 5, 9, 12
		3	MEH-3	1, 6, 12
		2	MEH-2	1, 12

CD: Conical Diffuser inlet. E: Elbow inlet. L: low water flow rate (6 L/min). H: high water flow rate (16 L/min).

3.2. Reliability of the VTC Method in the Determination of Temperature-Based Stratification Indicators When a Reducing Number of Experimental Measurement Points Are Used

It was intended to verify how the decrease in the number of temperature data points used (7, 4, 3 or 2, with respect to the initial 12 points) affects the consistency and usefulness of the models under different conditions of flow rate (6 L/min or 16 L/min) and inlet device (CD or E). With this aim, the models included in Table 2 were used, both for the characterization of the instantaneous temperature profile and for the estimation of the thermocline thickness evolution throughout charging.

According to the methodology proposed by Musser and Bahnfleth [22], a dimensionless cut-off temperature, referred to as Θ, was used to estimate the thermocline thickness. Then, giving to Θ the values 0.9 and 0.1, respectively, the remaining 80% of the total temperature gradient was considered to obtain the thermocline thickness at a given time.

Two different statistical parameters, namely the Pearson correlation coefficient (r) and the root mean square error ($RMSE$), were used for assessing the models' performance when estimating both the temperature evolution and thermocline thickness, which were defined as follows:

$$RMSE = \left(\frac{1}{n} \cdot \sum_{i=1}^{n} (x_i - \hat{x}_i)^2 \right)^{0.5} \tag{1}$$

$$r = \frac{n \sum x_i \hat{x}_i - (\sum x_i)(\sum \hat{x}_i)}{\sqrt{n(\sum x_i^2) - (\sum x)^2} \sqrt{n(\sum \hat{x}_i^2) - (\sum \hat{x}_i)^2}} \tag{2}$$

where x_i and $\hat{x}_i$ are the experimental and estimated values of temperature or thermocline thickness, respectively, and n is the number of observations.

3.3. Comparison between VTC Method When Using Fewer Measurement Points and a 3D-CFD Model. Practical Application to the Estimation of the Instantaneous Temperature Profile

In a previous publication [10], CFD techniques were applied to the study of thermal stratification during charging in the same facility used in the present study. Thus, three-dimensional Unsteady Reynolds-Averaged Navier–Stokes (URANS) simulations were carried out with the commercial software STAR-CCM+, ver. 6.04.014 (CD-Adapco,

Siemens Digital Industries Software) [30]. The model was based on the mass and momentum conservation equations and on a finite-volume method for solving the Navier–Stokes equations [31]. To ensure the conservation of mass, a standard pressure correction algorithm (SIMPLE) was used. A standard two-layer k-ε model, which offers the most mesh flexibility, was selected, solving the incompressible Navier–Stokes equations in integral form for continuity and momentum.

Regarding the boundary conditions, the inflow was set using a uniform velocity profile, while a convective condition was applied for the outflow. The incoming water temperature was set at 325.7 K.

Concerning the mesh, several structured grids were developed and tested to check the grid dependency of the solution. In the water body, a structured grid of 1,506,840 cells was selected based on a sensitivity analysis that considered comparison between simulations and experiments, convergence criteria and simulation time. The Grid Convergence Index (GCI), as calculated in Celik et al. [32], was used to estimate the convergence error. The maximum GCI was 0.01% between the selected grid and the finer one. The geometrical variation between cells was kept to a value of around 4%. A structured grid was also defined for the steel (tank wall) and fiberglass (insulating material) domains, and the same procedure was followed to verify the grid dependency of the solution.

The simulations were validated with the four thermal charging tests shown in Table 1. The validation was performed by comparing the evolution of the water temperature at each thermocouple position inside the tank determined experimentally and estimated from the CFD model, and a high correlation was found between experimental and numerical results. Three different statistical parameters, specifically the mean squared error MSE (K2), the root mean square error *RMSE* (K) and the relative error RE (%), were used to determine error rates.

To compare the CFD results with those obtained with the methodology proposed in this paper (VTC when using a minimum number of measurement points) in a practical way, the temperature profile was determined with both techniques at a given time during thermal charge.

4. Results and Discussion

4.1. Sensitivity of the VTC Method to the Decrease in the Experimental Temperature Data Points Used
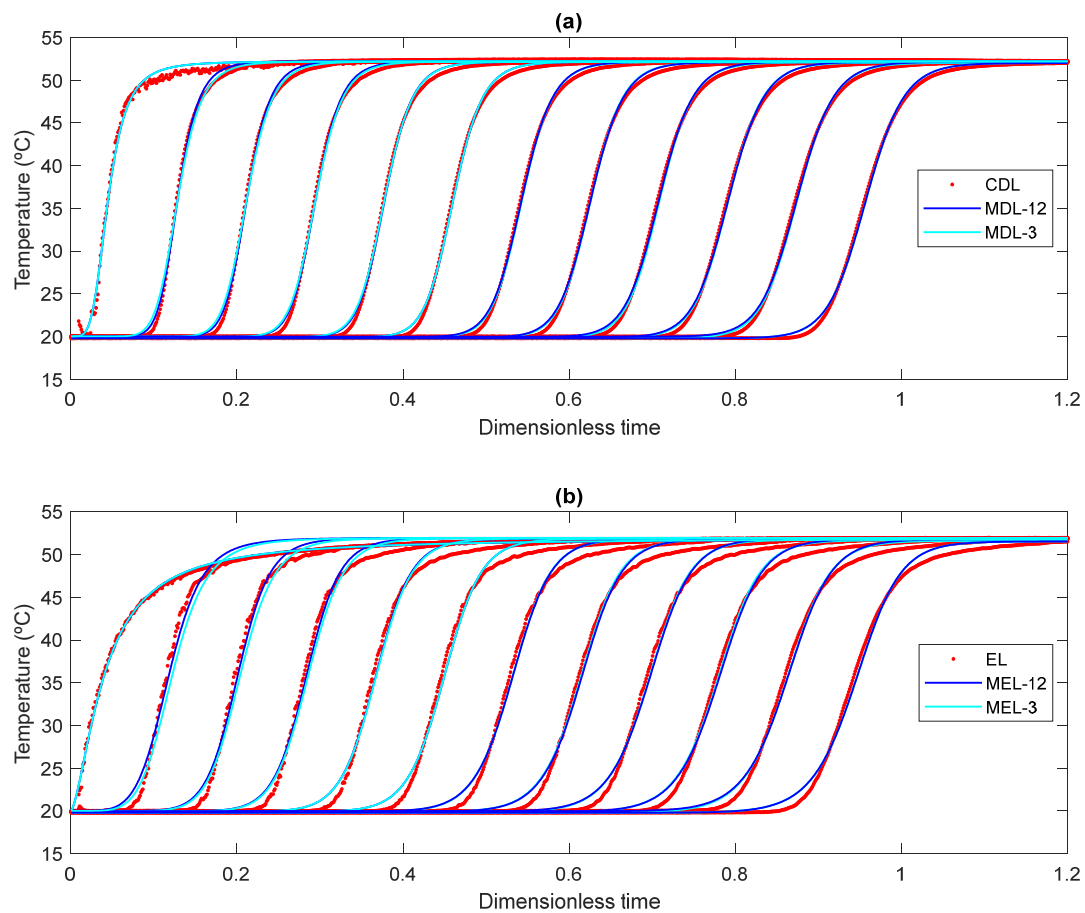
Figure 3 shows the temperature profile evolution at each TC location, estimated from the experimental data with the CD inlet (Figure 3a) and with the Elbow inlet (Figure 3b), both at a low flow rate. In addition to experimental data (CDL and EL), the corresponding models performed with 12 TC (MDL-12 and MEL-12) and 3 TC (MDL-3 and MEL-3) are also depicted. As can be seen in Figure 3a,b, the temperature at the location of each real TC during charging showed a similar trend in both the experimental tests and with the methods performed with 12 and 3 real TC. A good correspondence between the experimental and estimated temperature values was found. The results obtained with the CD at a high flow rate showed a similar pattern. However, it was not the case with the E inlet at a high flow rate.

The results obtained when estimating the temperature with 7 TC (MDL-7 and MEL-7) and with 4 TC (MDL-4 and MEL-4) are not shown graphically since they showed much less appreciable differences and matched the experimental values better than those obtained with 3 TC, as expected.

Table 3 shows the *RMSE* values (in °C) obtained for each model in the estimation of the temperature evolution at the 12 TC locations during the charging process.

The *RMSE* values in the temperature estimations with MDL, MDH and MEL models were, on average, less than 0.6 °C and 0.87 °C at most, MEL-2 being the worst case. The errors with MEH models were higher, with an average *RMSE* less than 4.39 °C and a maximum of 11.91 °C in MEH-3. Thus, very good accuracy in the prediction of the temperature evolution in the usual operating conditions of solar hot water tanks was found. On the other hand, a very slight worsening in the model accuracy was found when the

number of TC used in the models decreased. Moreover, the accuracy of the models also depended on the water flow, the errors in the cases with low flow rates (MDL and MEL models) being lower than in the rest.

Figure 3. Temperature profile evolution at each TC position. Results with CD (**a**) and E (**b**), both at low flow rate: experimental data, models with 12 TC and models with 3 TC.

Regarding the Pearson correlation coefficient (*r*), the data are not detailed in a table because very similar values were found in all cases. It should be noted that, with MDL and MDH (models with an inlet through the CD both at high and low flow rates), as well as with MEL (models with an inlet through the elbow at low flow rate), the value of the coefficient *r* was always (in all TC) greater than 0.99. Conversely, with MEH (models with an inlet through the elbow at a high flow rate), this value dropped to 0.69, confirming a weak correlation between experimental and estimated temperature values under these conditions. It should be noted that the models that provided a good estimate of the temperature evolution were those with a Re < 10,000 at the inlet devices (MDL, MDH and MEL models). Conversely, MEH models with a Reynolds number at the inlet significantly higher than the rest (Re = 24,489.1) did not give acceptable results.

In view of these results, it can be stated that by reducing the number of TC used in experimental tests to three, the VTC procedure allows estimation of the temperature evolution at any height in the tank located between the thermocouples used for making the estimation with great accuracy. It was found that it is even possible to use the data provided by only 2 TC (minimum number of TCs in the models proposed in this work), which could be placed near the inlet and outlet, assuming the small increase in error that occurs. It is important to highlight that the method is valid if applied under operating conditions with no excessive turbulence at the inlet.

Table 3. *RMSE* (°C) values obtained for each model in the estimation of the temperature evolution at the 12 TC locations.

Inlet Device	Flow Rate	Model	RMSE (°C)		
			Min	**Max**	**Mean ± SD**
CD	L	MDL-12	0.2065	0.3525	0.2344 ± 0.0391
		MDL-7	0.2065	0.3525	0.2403 ± 0.0385
		MDL-4	0.2065	0.3525	0.2488 ± 0.0438
		MDL-3	0.2065	0.3525	0.2511 ± 0.0475
		MDL-2	0.2065	0.5765	0.3776 ± 0.1306
CD	H	MDH-12	0.2726	0.4861	0.4168 ± 0.0519
		MDH-7	0.2726	0.5199	0.4254 ± 0.0597
		MDH-4	0.2726	0.4963	0.4148 ± 0.0570
		MDH-3	0.2726	0.5306	0.4155 ± 0.0583
		MDH-2	0.2726	0.5560	0.4059 ± 0.0626
E	L	MEL-12	0.2500	0.6934	0.4986 ± 0.0988
		MEL-7	0.2500	0.7422	0.5060 ± 0.1086
		MEL-4	0.2500	0.7664	0.5080 ± 0.1148
		MEL-3	0.2500	0.7897	0.5057 ± 0.1243
		MEL-2	0.2500	0.8706	0.5680 ± 0.1676
E	H	MEH-12	0.5358	1.1627	0.9370 ± 0.1772
		MEH-7	0.6696	2.2961	1.1065 ± 0.4039
		MEH-4	0.8582	3.5876	1.6722 ± 0.9011
		MEH-3	0.8582	11.9128	4.3881 ± 3.5252
		MEH-2	0.8582	5.7062	3.9027 ± 1.7227

SD: Standard deviation. CD: Conical Diffuser inlet. E: Elbow inlet. L: low water flow rate (6 L/min). H: high water flow rate (16 L/min).

Arias et al. [33] investigated, by means of simulations, the sensibility of the long-term performance of solar energy systems equipped with an HWST to the number of discrete sections or nodes used to model the storage system temperature distribution and the degree of stratification. Their findings diverge from those reported here as the research approach showed significant differences. The authors simulated a complete solar domestic water heating system over a long period of time (one year), considering the effect of the annual variability in climatic conditions (solar fraction). In addition, the influence of several system parameters (e.g., tank size, collector flow rate, etc.) on the sensitivity of the results to the number of nodes was analyzed, and simulations were carried out with different time steps. They concluded that in long-term simulations, the level of detail in which the temperature inside the tank is represented is less important than the overall energy balance on the system. Therefore only a small number of nodes (five in the case study) are needed to accurately simulate the annual performance of a solar system, this result being not applicable in short-term simulations or experiments as those reported in the present paper.

4.2. Reliability of the VTC Method in the Determination of Temperature-Dependent Stratification Indices When a Reducing Number of Experimental Measurement Points Are Used

4.2.1. Applying the VTC Method with Fewer Measurement Points to Temperature Profile Characterization

The temperature profile obtained with all the MEL, MDL and MDH models was well defined and showed great agreement with that obtained from experimental data, regardless of the number of TC used for its determination. Figure 4 shows the instantaneous temperature profile at t* = 0.5058 (50.58% of the total tank volume replaced) obtained with the experimental data in the CDL test and the five MDL models.

As can be observed, the results obtained with the five models were very similar, although the model accomplished with two measuring points (MDL-2) showed slightly less accuracy in the region between thermocouples 5 and 8, which coincide in this case

with the zone where there is an important and abrupt change in temperature in a very small space (thermocline gradient region).
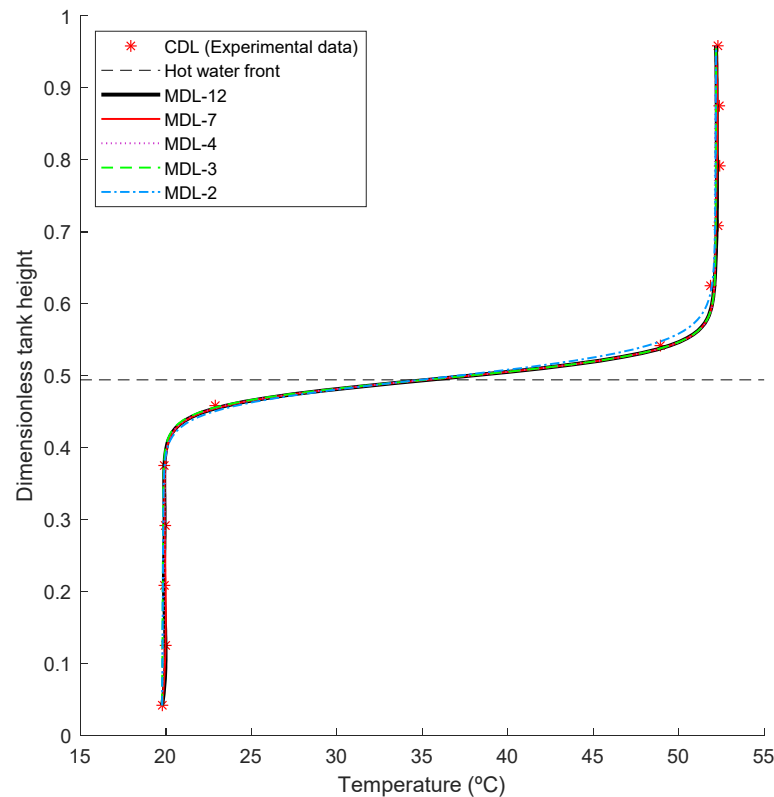
Figure 4. Instantaneous temperature profile at t* = 0.5058 (50.58% of the total tank volume replaced) in CD at low flow rate. Experimental data (CDL) and results derived from the five MDL models which used the data provided from 12, 7, 4, 3 and 2 TC, respectively.

4.2.2. Applying the VTC Method with Fewer Measurement Points to Estimate Thermocline Thickness

Figure 5 shows the evolution of the thermocline thickness estimated with the two inlet devices and the two flow rates at the points where the TCs were located, using the data recorded by 12, 7, 4, 3 and 2 TCs. As can be seen, the method worked correctly under the usual operating conditions in this type of tank (MDL, MDH and MEL) but not so much under conditions of excessive turbulence at the inlet (MEH). The elbow with a high flow rate did not yield satisfactory results due to the mixing produced by the turbulence generated at the inlet, as demonstrated by García-Marí et al. [28]. In accordance with Zurigat and Ghajar [19], the hydrodynamic and thermal characteristics of the flow could be detrimental to the formation of a thin thermocline in this case.

It was proven that in the MDL, MDH and MEL cases, the evolution of the dimensionless thermocline thickness was quite similar in the models performed with more than two TC (Figure 5). Furthermore, the greatest differences found when determining the evolution of the thermocline thickness using less than 12 TC, with respect to that estimated with the 12 measurement points, occurred at the beginning of the thermal charge. The zone where these greatest differences were detected coincided with the region in which the evolution of temperature during charging was the worst fit with the sigmoidal shape (Figure 3).

The evolution of the instantaneous temperature profile estimated with the five models of both MEL and MDH cases during the charging period is depicted in two videos available as Supplementary Materials (Video 1 with MEL models and Video 2 with MDH models). Simultaneous with the evolution of temperature profiles, the evolution of thermocline thickness during the same period is displayed in a separate frame also for all MEL

(Video 1) and MDH (Video 2) models. These videos intend to visualize the results shown in Figures 4 and 5 in a dynamic, intuitive and more detailed way, as discussed below.
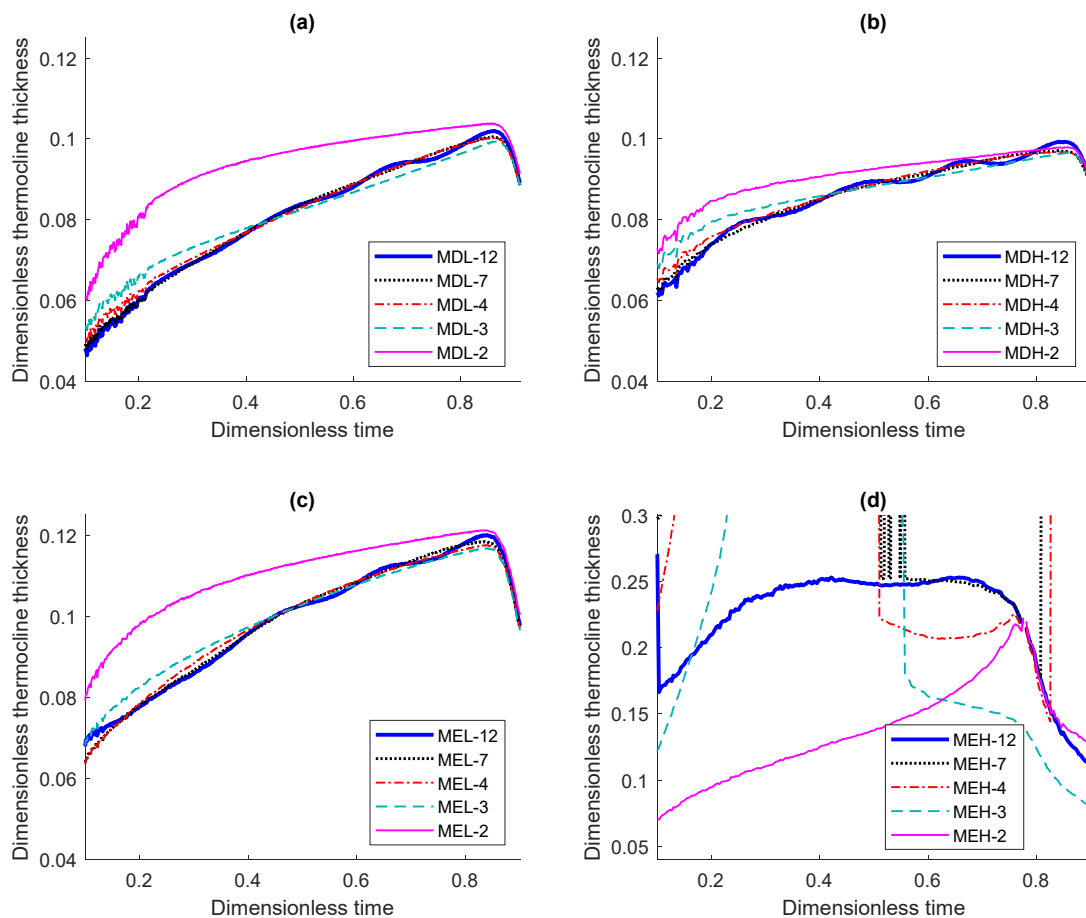
Figure 5. Evolution of the thermocline thickness at the points where the thermocouples were located. Estimation with MDL (**a**), MDH (**b**), MEL (**c**) and MEH (**d**) models.

In the videos, the thermocouples used in each model (see Figure 2) were highlighted with a red circle. According to [19], once the thermocline is formed, it travels down as the charging continues until it is destroyed, indicating full charge. It is observed that the temperature estimation at the locations of the thermocouples not used in each model (thermocouples not highlighted with the red circle) is very precise and differs very little from the ones that were actually registered.

Table 4 shows the *RMSE* values (°C) in the estimation of thermocline thickness at the TC locations calculated with 7, 4, 3 and 2 TC, with respect to those calculated with 12 TC in MDL, MDH, MEL and MEH. The maximum difference (expressed as a percentage) between the thermocline thickness determined with 12 TC, compared to that determined with 7, 4, 3 and 2 TC, respectively, in MDL, MDH, MEL and MEH, is presented in Table 5. The Reynolds number at the inlet device is also depicted in both Tables 4 and 5.

Table 4. *RMSE* (°C) in the estimation of thermocline thickness at the TC locations calculated with 7, 4, 3 and 2 TC with respect to those calculated with 12 TC in MDL, MDH, MEL and MEH.

Models	*RMSE*_7TC (°C)	*RMSE*_4TC (°C)	*RMSE*_3TC (°C)	*RMSE*_2TC (°C)	Re (-)
MDL	0.00060	0.00104	0.00292	0.01505	1898.6
MDH	0.00091	0.00113	0.00247	0.00565	5062.9
MEL	0.00073	0.00131	0.00276	0.01312	9183.4
MEH	0.23932	0.21410	0.23085	0.10208	24,489.1

Table 5. Maximum difference (%) between the thermocline thickness determined with 12 TC compared to that determined with 7, 4, 3 and 2 TC, respectively, in MDL, MDH, MEL and MEH.

Models	Maxdif%_7TC	Maxdif%_4TC	Maxdif%_3TC	Maxdif%_2TC	Re (-)
MDL	1.39	2.81	6.60	21.15	1898.6
MDH	1.84	3.55	7.37	12.28	5062.9
MEL	1.29	2.33	4.21	17.06	9183.4
MEH	278.86	266.38	196.00	51.74	24,489.1

Without considering the MEH models in the comparative analysis for the reasons already argued, the values shown in Tables 4 and 5 indicate that the evolution of the thermocline thickness determined with fewer measurement points was similar to that obtained with the 12 thermocouples available in this study.

When applying the VTC method with less than 12 TC, the *RMSE* values increased slightly, this increase (and therefore the error in the estimation) being higher the lower the number of thermocouples used. In any case, very small *RMSE* values were always obtained, with a maximum of 0.01505 °C in MDL-2 and a minimum of 0.00091 °C in MDH-7, the *RMSE* average value being 0.0039 °C.

The maximum difference (expressed as a percentage) between the thermocline thickness determined with 12 TC and that determined with 7, 4 and 3 TC was obtained with CD inlet at a high flow rate (MDH models, Table 5). Although the differences logically increased in all cases as the number of thermocouples used decreased, they were very acceptable. The worst cases were 1.84% (MDH-7), 3.55% (MDH-4) and 7.37% (MDH-3), compared to the determination with the model performed with 12 TC (MDH-12). With the use of 2 thermocouples, the differences moderately increased (MDL-2 being the most unfavorable model), with a maximum difference of 21.57% in the thermocline thickness compared to the determination with 12 TC (MDL-12).

In view of these results, it can be stated that by applying the VTC method with only 3 TC, it is possible to obtain the temperature profiles and thermocline thickness evolution throughout a charge cycle with great precision and without the result being affected by the instant in which it is determined. It should be noted that the determination of the thermocline gradient or the thermocline thickness is only applicable under constant inlet flow rate at a uniform temperature [19,20]. However, study and analysis under these operating conditions can be decisive when characterizing the thermal storage tank with a view to developing models that allow the improvement of the design of the tank geometry (e.g., aspect ratio), or inlet/outlet devices, leading to an optimal storage configuration.

4.3. Comparison between VTC Method When Using Fewer Measurement Points and a 3D-CFD model. Practical Application to the Estimation of the Water Temperature at a Given Time during Charging

The instantaneous temperature profile at t* = 0.5734 (57.34% of the total tank volume replaced) was obtained for CD at a low flow rate with the MDL-3 model, with the CFD model previously developed and validated, and with the experimental data (CDL), are shown on the left-hand side of Figure 6. The right-hand side shows the temperature distribution also at t* = 0.5734, and for CD at a low flow rate, obtained with the CFD approach, the temperature contours being presented in the symmetrical XZ-plane.

Very small differences were observed between the CFD and VTC models in Figure 6. CFD is undoubtedly a useful tool that allows the analysis of three-dimensional flows with high spatial and temporal resolution. With CFD approaches, very detailed insights and understanding of the behavior of the fluid are achieved, providing additional information as compared to experimental measurements. Nevertheless, it is noteworthy that CFD analysis is a computationally intensive and time-consuming technique, as it requires the completion of certain stages (geometry creation, mesh generation, the study of grid dependency of the results, fluid physics boundary conditions and model selection, validation, etc.). By contrast, it takes very little time to perform an analysis with the VTC method and obtain an instantaneous temperature profile with good accuracy, as shown in Figure 6.
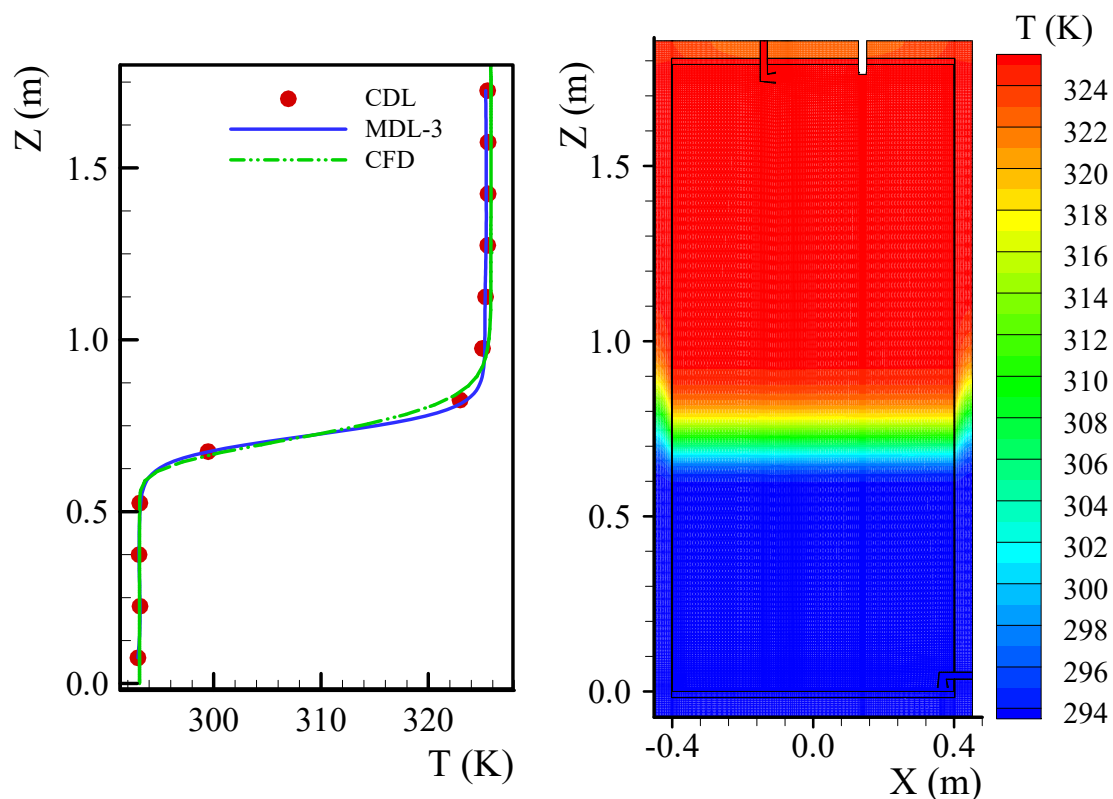
Figure 6. Left side: Instantaneous temperature profile at t* = 0.5734 obtained for CD at low flow rate with MDL-3 model (blue line), the CFD model (green dashed line) and the experimental data (CDL, red marker). **Right side**: Temperature distribution also at t* = 0.5734 and for CD at low flow rate, obtained with CFD.

It can be stated that the VTC method is complementary to other techniques, as from a few experimental points, the temperature value can be extrapolated to many other points that can be used both for validation of CFD simulations and for calculating temperature-dependent stratification indices.

5. Conclusions

This study evaluated the sensitivity of the VTC method developed by González-Altozano et al. [27] to a decrease in the number of temperature data points employed to assess the thermal performance of an HWST. It also determined the minimum number of experimental temperature data (number of thermocouples used) that allows the estimation of the temperature at any point and instant without affecting the accuracy or the quality of the results.

The facility and experimental tests described in González-Altozano et al. [27] were also used in the present work. Thus, four experimental tests were conducted in a 950-L tank during the charging process, in which two different inlet devices (elbow, E and conical diffuser, CD) and two water flow rates (high, H and low, L) were tested, and the water temperature was recorded with 12 thermocouples evenly placed along the tank's vertical axis.

Four models were developed for each experimental test, with the data recorded by 7, 4, 3 and 2 TC, respectively. The temperature values at the locations of the TC not used in each model were estimated by extrapolating the parameters of the 5PL function at these points. The results of the four models were compared with a fifth model performed for each experimental test with the data provided by the 12 TC. A total of 20 models were performed.

The temperature profile evolution at the TC locations, when estimated with 7, 4 and 3 TC, using MDL, MDH and MEL models, showed a pattern similar to the respective

determinations with 12 TC. The *RMSE* values in the temperature estimations with these models were, on average, less than 0.6 °C and, at most, 0.87 °C, with MEL-2 being the worst case. The differences found in MEH models were higher due to the greater turbulence generated with the E inlet at a high flow rate, with an average *RMSE* less than 4.39 °C and a maximum of 11.91 °C in MEH-3. The values of the Pearson correlation coefficient (*r*) were uniform in all cases, being higher than 0.99 in all TC of the MDL, MDH and MEL cases. It was, therefore, verified that by reducing the number of TC used in experimental tests to three, the VTC procedure allows estimation of the temperature in the tank with great accuracy. These 3 TC could be located next to the entrance, close to the exit, with the third somewhere between them. It was found that it is even possible to use the data provided by only 2 TC, which could be placed near the inlet and outlet, assuming a small increase in error. It is noteworthy that models which yielded good results were those with Re < 10,000 at the inlet devices.

To verify the suitability of the procedure using a smaller number of measurement points, its application to the estimation of both the instantaneous temperature profile and the thermocline thickness evolution throughout the charge cycle was carried out. Thus, the instantaneous temperature profile obtained using the data provided by 7, 4, 3 and even 2 TC, gave excellent results except for MEH models, showing a great correspondence with experimental data. Concerning the determination of the thermocline thickness, the method also yielded very acceptable results under the usual working conditions in this type of tank (MEL, MDL and MDH models). The dimensionless thermocline thickness was similar in the models performed with more than 2 TC, the greatest differences being found with respect to those estimated with the 12 measurement points observed at the beginning of the thermal charge. Very small *RMSE* values were always obtained, with a maximum of 0.01505 °C in MDL-2 and a minimum of 0.00091 °C in MDH-7, the *RMSE* average value being 0.0039 °C. The maximum differences in thermocline thickness value compared to the determination with 12 TC (expressed as a percentage) increased as the number of TC used decreased, with maximum values in the MDH models: 1.84% (MDH-7), 3.55% (MDH-4) and 7.37% (MDH-3). The most unfavorable model was MDL-2, which showed a maximum difference of 21.7%.

Finally, the comparison between the VTC method with a reducing number of measurement points and a 3D-CFD approach developed in a previous study was performed, and very small differences were observed between both models when applied to the estimation of the instantaneous temperature profile.

In view of the above, the main conclusions arising from this study are as follows.

The VTC model, implemented with as few as 2 or 3 experimental temperature data measurements, results in a suitable method for the analysis of the thermal performance and for the determination of several of the temperature-based indices used to quantify the stratification efficiency in HWSTs during thermal charge.

Under usual working conditions (with no excessive turbulence at the inlet, Re < 10,000), the virtual TC method provides these estimations with more spatial precision and temporal stability than other methods. On the other hand, the validity of the obtained results is limited to experimental conditions in which the initial temperature inside the tank is uniform and with water flow rate and the temperature kept constant during thermal charge. However, the study and analysis under these operating conditions can be decisive in characterizing the thermal storage tank with a view to developing models that allow improvement of the design of the tank geometry (e.g., aspect ratio), or inlet/outlet devices, leading to an optimal storage configuration.

It is also important to point out that the proposed methodology may be a complementary tool to other techniques or methods, as from a few experimental points and requiring low experimental resources and time, the temperature values can be extrapolated to many other points. Therefore, it could be employed both for validation of numerical simulations and also to properly evaluate the thermal performance in cases where only a few experimental values are available.

Nomenclature

4PL	Four-parameter logistic function
5PL	Five-parameter logistic function
CFD	Computational Fluid Dynamics
MDH	Models performed with the conical diffuser inlet at high water flow rate
MDL	Models performed with the conical diffuser inlet at low water flow rate
E	Elbow
MEL	Models performed with the elbow inlet at low water flow rate
MEH	Models performed with the elbow inlet at high water flow rate
H	High water flow rate (L/min)
HWST	Hot water storage tank
LI	Linear interpolation
L	Low water flow rate (L/min)
r	Pearson's correlation coefficient
Re	Reynolds number (-)
RMSE	Root Mean Square Error (°C)
CD	Conical diffuser
t*	Dimensionless time
TC	Thermocouple
VTC	Virtual TC
Greek letters	
Θ	Dimensionless temperature

References

1. Cruickshank, C.A.; Baldwin, C. Sensible thermal energy storage: Diurnal and seasonal A2. In *Storing Energy*, 1st ed.; Letcher, T.M., Ed.; Elsevier: Amsterdam, The Netherlands, 2016; pp. 291–311. [CrossRef]
2. Njoku, H.O.; Ekechukwu, O.V.; Onyegegbu, S.O. Analysis of stratified thermal storage systems: An overview. *Heat Mass Transf.* **2014**, *50*, 1017–1030. [CrossRef]
3. Fertahi, S.; Jamil, A.; Benbassou, A. Review on solar thermal stratified storage tanks (STSST): Insight on stratification studies and efficiency indicators. *Sol. Energy* **2018**, *176*, 126–145. [CrossRef]
4. Chandra, Y.P.; Matuska, T. Stratification analysis of domestic hot water storage tanks: A comprehensive review. *Energy Build.* **2019**, *187*, 110–131. [CrossRef]
5. Deng, J.; Furbo, S.; Kong, W.; Fan, J. Thermal performance assessment and improvement of a solar domestic hot water tank with PCM in the mantle. *Energy Build.* **2018**, *172*, 10–21. [CrossRef]
6. Erdemir, D.; Atesoglu, H.; Altuntop, N. Experimental investigation on enhancement of thermal performance with obstacle placing in the horizontal hot water tank used in solar domestic hot water system. *Renew. Energy* **2019**, *138*, 187–197. [CrossRef]

7. Zhang, Z.; Song, P.; Fan, Y. Experimental investigation on the geometric structure with perforated baffle for thermal stratification of the water tank. *Sol. Energy* **2020**, *203*, 197–209. [CrossRef]

8. Chandra, Y.P.; Matuska, T. Numerical prediction of the stratification performance in domestic hot water storage tanks. *Renew. Energy* **2020**, *154*, 1165–1179. [CrossRef]

9. Bouhal, T.; Fertahi, S.; Agrouaz, Y.; El Rhafiki, T.; Kousksou, T.; Jamil, A. Numerical modeling and optimization of thermal stratification in solar hot water storage tanks for domestic applications: CFD study. *Sol. Energy* **2017**, *157*, 441–455. [CrossRef]

10. Moncho-Esteve, I.J.; Gasque, M.; González-Altozano, P.; Palau-Salvador, G. Simple inlet devices and their influence on thermal stratification in a hot water storage tank. *Energy Build.* **2017**, *150*, 625–638. [CrossRef]

11. Wang, Z.; Zhang, H.; Dou, B.; Huang, H.; Wu, W.; Wang, Z. Experimental and numerical research of thermal stratification with a novel inlet in a dynamic hot water storage tank. *Renew. Energy* **2017**, *111*, 353–371. [CrossRef]

12. Gasque, M.; González-Altozano, P.; Maurer, D.; Moncho-Esteve, I.J.; Gutiérrez-Colomer, R.P.; Palau-Salvador, G.; García-Mari, E. Study of the influence of inner lining material on thermal stratification in a hot water storage tank. *Appl. Therm. Eng.* **2015**, *75*, 344–356. [CrossRef]

13. Pizzolato, A.; Donato, F.; Verda, V.; Santarelli, M. CFD-based reduced model for the simulation of thermocline thermal energy storage systems. *Appl. Therm. Eng.* **2015**, *76*, 391–399. [CrossRef]

14. Nicotra, M.; Caldera, M.; Leone, P.; Zanghirella, F. Model-based analysis of thermal energy storage for multiple temperature level heat supply. *Appl. Therm. Eng.* **2018**, *141*, 288–297. [CrossRef]

15. Haller, M.Y.; Cruickshank, C.A.; Streicher, W.; Harrison, S.J.; Andersen, E.; Furbo, S. Methods to determine stratification efficiency of thermal energy storage processes—Review and theoretical comparison. *Sol. Energy* **2009**, *83*, 1847–1860. [CrossRef]

16. Castell, A.; Medrano, M.; Solé, C.; Cabaza, L.H. Dimensionless numbers used to characterize stratification in water tanks for discharging at low flow rates. *Renew. Energy* **2010**, *35*, 2192–2199. [CrossRef]

17. Mawire, A.; Taole, S.H. A comparison of experimental thermal stratification parameters for an oil/pebble-bed thermal energy storage (TES) system during charging. *Appl. Energy* **2011**, *88*, 4766–4778. [CrossRef]

18. Rendall, J.; Abu-Heiba, A.; Gluesenkamp, K.; Nawaz, K. Nondimensional convection numbers modeling thermally stratified storage tanks: Richardson's number and hot-water tanks. *Renew. Sustain. Energy Rev.* **2021**, *150*, 111471. [CrossRef]

19. Zurigat, Y.; Ghajar, A. Heat transfer and stratification in sensible heat storage systems. In *Thermal Energy Storage. Systems and Applications*; Dinçer, I., Rosen, M.A., Eds.; John Wiley & Sons: Hoboken, NY, USA, 2002; pp. 259–301.

20. Bahnfleth, W.P.; Song, J. Constant flow rate charging characteristics of a full-scale stratified chilled water storage tank with double-ring slotted pipe diffusers. *Appl. Therm. Eng.* **2005**, *25*, 3067–3082. [CrossRef]

21. Yoo, J.; Wildin, M.; Truman, C.R. Initial formation of a thermocline in stratified thermal storage tanks. *ASHRAE Trans.* **1986**, *92*, 280–292.

22. Musser, A.; Bahnfleth, W.P. Evolution of temperature distributions in a full-scale stratified chilled-water storage tank with radial diffusers. *ASHRAE Trans.* **1998**, *104*, 1–13.

23. Chung, J.D.; Cho, S.H.; Tae, C.S.; Yoo, H. The effect of diffuser configuration on thermal stratification in a rectangular storage tank. *Renew. Energy* **2008**, *33*, 2236–2245. [CrossRef]

24. Dhahad, H.A.; Alaweea, W.H.; Habeeb, L.J. Numerical investigation for the discharging process in cold-water storage tank. *J. Mech. Eng. Res. Dev.* **2020**, *43*, 295–306.

25. Bonanos, A.M.; Votyakov, E.V. Sensitivity analysis for thermocline thermal storage tank design. *Renew. Energy* **2016**, *99*, 764–771. [CrossRef]

26. Wang, Z.; Zhang, H.; Huang, H.; Dou, B.; Huang, X.; Goula, M.A. The experimental investigation of the thermal stratification in a solar hot water tank. *Renew. Energy* **2019**, *134*, 862–874. [CrossRef]

27. González-Altozano, P.; Gasque, M.; Ibáñez, F.; Gutiérrez-Colomer, R.P. New methodology for the characterisation of thermal performance in a hot water storage tank during charging. *Appl. Therm. Eng.* **2015**, *84*, 196–205. [CrossRef]

28. García-Marí, E.; Gasque, M.; Gutiérrez-Colomer, R.P.; Ibáñez, F.; González-Altozano, P. A new inlet device that enhances thermal stratification during charging in a hot water storage tank. *Appl. Therm. Eng.* **2013**, *61*, 663–669. [CrossRef]

29. Bayón, R.; Rojas, E. Analytical function describing the behaviour of a thermocline storage tank: A requirement for annual simulations of solar thermal power plants. *Int. J. Heat Mass Transf.* **2014**, *68*, 641–648. [CrossRef]

30. CD-Adapco Inc. *STAR-CCM+User Guide*; CD-Adapco Inc.: Melville, NY, USA, 2011.

31. Versteeg, H.K.; Malalasekera, W. *An Introduction to The Computational Fluid Dynamics: The Finite Volume Method*; Longman Scientific and Technical: New York, NY, USA, 1998.

32. Celik, I.B.; Ghia, U.; Roache, P.J.; Freitas, C.J.; Coleman, H.; Raad, P.E. Procedure for estimation and reporting of uncertainty due to discretization in CFD applications. *J. Fluids Eng.* **2008**, *130*, 078001-1–078001-4.

33. Arias, D.A.; McMahan, A.C.; Klein, S.A. Sensitivity of long-term performance simulations of solar energy systems to the degree of stratification in the thermal storage unit. *Int. J. Energy Res.* **2008**, *32*, 242–254. [CrossRef]